CONF-800507--3

LA-UR -80-827

TITLE: THE INFLUENCE OF ORIENTATION ON FRACTURE TOUGHNESS AND TENSILE MODULI IN BERKELEY GRANITE

AUTHOR(S): P. M. Halleck and A. J. Kumnick*

MASTER

SUBMITTED TO: 21st U.S. National Symposium on Rock Mechanics
University of Missouri-Rolla
Rolla, Missouri
May 28-30, 1980

*Present address: Case Western Reserve University, Cleveland, OH

University of California

LOS ALAMOS SCIENTIFIC LABORATORY
Post Office Box 1663 Los Alamos, New Mexico 87545
An Affirmative Action/Equal Opportunity Employer

Form No. 836 R3
St. No. 2629
12/78

UNITED STATES
DEPARTMENT OF ENERGY
CONTRACT W-7405-ENG. 36

DISCLAIMER

DISCLAIMER

Portions of this document may be illegible in electronic image products. Images are produced from the best available original document.

THE INFLUENCE OF ORIENTATION ON FRACTURE TOUGHNESS AND TENSILE MODULI IN BERKELEY GRANITE

By

P. Halleck and A. J. Kumnick

Geosciences Division

Los Alamos Scientific Laboratory

Los Alamos, NM 87545

ABSTRACT

Fracture toughness and tensile modulus values for Berkeley granite show pronounced orientation dependence. Apparent fracture toughness values (K_Q) correspond to natural strong and weak planes in the rock: cracks propagated in the head grain (strongest) plane have K_Q = 1.81 MPa $\sqrt{m}$, those grown in the rift (weakest) plane have K_Q = 1.01 MPa $\sqrt{m}$ and those in the grain (intermediate) plane have K_Q = 1.40 MPa $\sqrt{m}$. These directional K_Q data also correlate with tensile modulus values, E, which are 50.7 GPa, 21.6 GPa, and 39.3 GPa respectively. An empirical relationship between K_Q and E is demonstrated. Monitoring of acoustic emission events shows promise as a detector of onset of crack growth.

INTRODUCTION

During recent years awareness of need for inexhaustible energy resources has focused attention on the development of hot dry rock (HDR) geothermal energy [1]. This new technique involves extraction of heat from hot crustal rocks by creating an artificial hydrothermal system. Currently a feasibility study involving the formation of a reservoir for underground heat extraction in low-permeability, granitic basement rock is underway on the Jemez Plateau about 30 km (18.6 mi) west of Los Alamos, New Mexico under direction of the Los Alamos Scientific Laboratory (LASL)[2]. The technique being studied uses hydraulic fracturing to produce a flow connection between two drilled holes at depths from 3 to 5 km . Large fracture surface areas are required because the rock surrounding the fracture conducts heat rather poorly and quickly controls the rate of heat transfer to the circulating fluid contained in the fracture zone.

Because the nature and extent of the fracture are vitally important to the heat exchange process, quantitative knowledge of the behavior of granite is required for the design of an optimal system. In addition to predicting the extent of the initial hydraulic fracture, reliable fracture properties are needed for predicting stability of the fracture over the (20 year) lifetime of an HDR reservoir and for modeling possible thermal stress cracking in the reservoir, which may affect heat transfer rates. The present investigation of orientation dependence of fracture toughness was aimed at improving our understanding of fracture growth and stability in granite in support of the LASL HDR program.

Test Material

The rock used in this investigation is Berkeley granite from Georgia, selected for its small (~0.5-mm) grain size and availability in large sample size. Physical and mechanical properties and modal analyses are shown in Table 1. The following results are based on samples cut from a single 0.2-m^3 block and oriented in orthogonal directions using the single polished face as a reference plane (Fig. 1). Sample nomenclature is arranged such that fracture propagation is in the plane for which the sample is named. Fracture toughness and tensile modulus specimens were cut in pairs. Tensile loading is arranged perpendicular to the fracture growth plane of the corresponding fracture toughness specimens.

Experimental Methods

Specimens for three-point-bend fracture toughness testing (Fig. 2) were cut from each orientation 25 mm x 12 mm x 150 mm (Fig. 1) using a diamond saw. Top and bottom surfaces were ground parallel to within 0.025 mm (0.001 in.). A starter crack of depth 2.5 - 6.0 mm (0.1 - 0.25 in.) was cut into each specimen using a wire saw, which was fitted with 0.20-mm

TABLE I

Density:	2.63×10^3 kg/m^3 (164 lb/ft^3)	
Porosity:	0.66%	
Modal Analysis:*	Mineral	Percent by Volume
	Quartz	27.5
	Alkali Feldspar	34.0
	Potassium Feldspar	26.2
	Biotite	5.1
	Muscovite	4.1
	Other	3.1
		100.0

*Average of separate analyses by Eddy [3] and by Sykes [4]. Sykes performed analyses on three orthogonal sections finding no significant differences with orientation.

(0.008-in.) diamond impregnated steel wire. Samples were loaded in an Instron servo-mechanical testing machine.

Crack growth was monitored by measuring crack opening displacement (COD) with a 0.25-mm-range linear

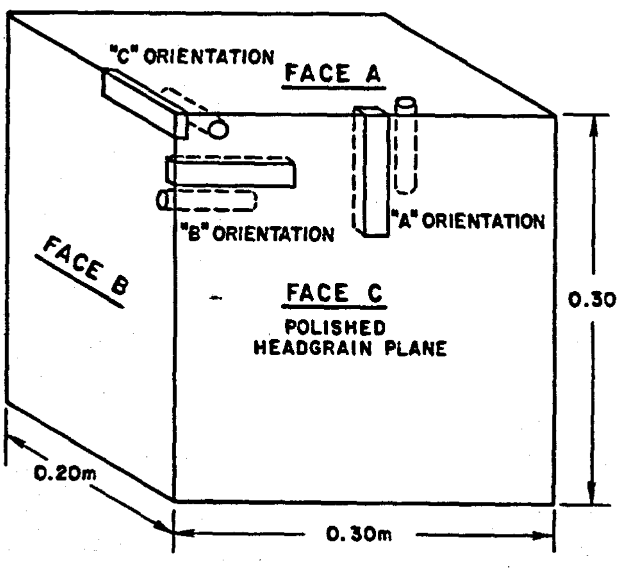

Figure 1. Orientation and nomenclature of fracture toughness and tensile modulus specimens relative to the quarried surfaces of the Berkeley Granite test block.

variable differential transformer (LVDT) gauge head mounted as shown in (Fig. 2). The relationship between COD and crack length was established using the compliance calibration procedure (Schmidt [5]) in which artificial "cracks" are sawn to a given depth in a test sample. At each depth, the initial slope of the load vs. COD curve is used to calculate an effective compliance, $C = b\Delta M/S$, where b is the sample thickness, and $\Delta M/S$ is the reciprocal of the initial slope. This is plotted vs. the relative crack length, a/W, where a is the crack length and W is the sample width. During actual fracture toughness tests, the effective compliance for each load cycle is determined and compared to this calibration data to deduce the crack length.

In the present tests, the loading behavior was non-linear making a unique determination of effective compliance impossible (Fig. 3). We attribute this behavior to interference between fractured surfaces which prevents complete closure and resists reopening of a crack. The unloading portions of each cycle were, however, highly linear and were used to estimate crack length for the succeeding cycle.

Cracks were always grown 2.5 - 5 mm (0.1-0.2 in.) away from the saw cut (using from one to three loading cycles) before any fracture toughness data were recorded. This procedure minimizes the effects of local damage which may have been introduced by wire sawing, and assures "natural" crack tip geometry.

Typically, several fracture toughness values were obtained for each specimen by unloading as soon as steady crack growth occurred. The applied load was slowly raised (constant load line displacement rate =

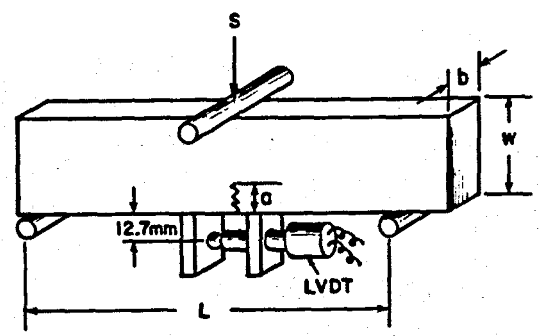

Figure 2. Diagram of experimental arrangement. For these tests L = 96.5 mm, b Z 12.5 mm, W Z 25.4 mm.

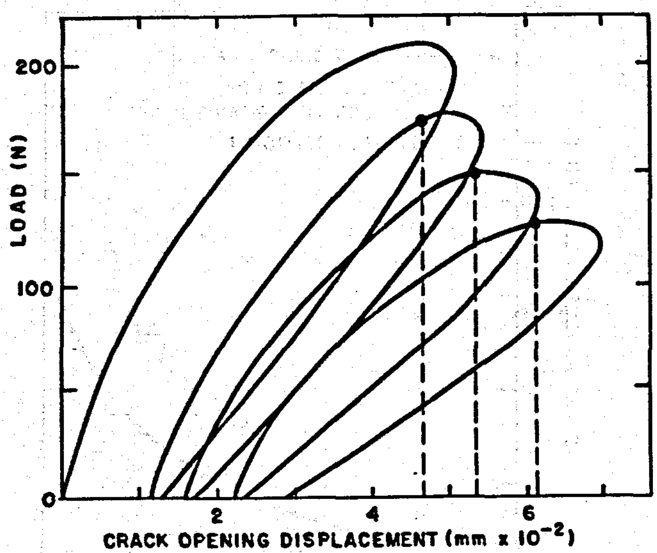

Figure 3. Typical loading cycles showing load as a function of crack opening displacement (COD). The dark circles represent the onset of steady crack growth as determined by acoustic emission (see Fig. 8).

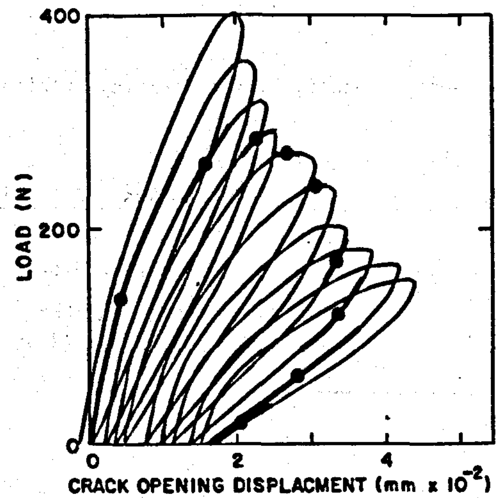

Figure 4. Acoustic emission frequency signature test. The ratio of high frequency (0.3 - 1.0 MH_Z) to low frequency (<0.1 MH_Z) counts was measured over the darkened segment of successive loading cycles. The dark circle represents the median load of the data collection range for each cycle (see Fig. 9).

8.5×10^{-4} mm/sec) until a maximum load was reached, then decreased to zero. Values of critical load (PQ) and crack length (a/W) were determined for each cycle from the resulting plot of load vs. COD.

During a number of fracture toughness tests, acoustic emission events were monitored using a Model 920 Dunegan/Endevco system. Attempts were made to distinguish frequency signatures for various phases of crack opening and growth, and to correlate event rate with the onset of crack growth. The signal from a single, broad-band transducer was amplified and filtered by two separate systems, one with a 100 KHz low-pass frequency range and the other with a 300 KHz to 1 MH_Z band-pass range. Background noise was minimized by setting a minimum recording threshold. Ratios of high frequency to low frequency counts were monitored over small portions of successive loading cycles (Fig. 4), and compared to the stress intensity factor normalized to the measured K_Q (see below). In addition, cumulative low frequency events were plotted versus the incremental crack mouth opening during individual cycles. Correlations of event rate with crack growth were made in this manner.

The tensile moduli $E = \sigma/\epsilon$ were measured perpendicular to each plane on 26-mm-diameter, right-circular cylinders pulled in tension. These were cut with a diamond core drill in the directions shown in Fig. 1. The four-arm bridge circuit used consisted of two active strain gauges mounted on each sample and two additional passive gauges mounted in an unstrained identical sample. The samples were gripped via steel holders epoxied to each end and loaded through swivel platens. Secant moduli were calculated between zero and maximum stress of approximately 3.1 MPa (450 psi).

RESULTS AND DISCUSSION

The results of the compliance calibrations for each orientation are shown in Fig. 5. To test their validity, these data were converted to dimensionless form by multiplying by the tensile modulus and compared with both the analytic solution of Jones and Brown [6], and experimental data on cold rolled steel specimens of the same geometry. Tensile moduli for Berkeley Granite were measured as described above with results as shown in Table II. The tensile modulus for the steel was calculated from its measured density of 7.887×10^3 kg/m^3 and longitudinal sound speed of 5.36 km/sec, to be 2.27×10^2 GPa (3.29×10^7 psi).

The analytical compliance curve CE vs. a/W (Fig. 6) is lower than the experimental one by a factor of about 2 for both granite and steel specimens. The discrepancy is due to the mechanical amplification of

TABLE II

Tensile moduli, E, for Berkeley Granite

Sample Orientation	Modulus (GPa, psi x 10^6)
A	39.3 ± 2.2 (5.70 ± 0.31)
B	21.6 ± 1.0 (3.14 ± 0.14)
C	50.7 ± 2.5 (7.36 ± 0.36)

COD as a result of placing the LVDT 12.7 mm (0.5 in.) below, rather than flush with the sample surface. To verify this, the steel was remeasured using a second COD gauge mounted flush with the lower sample surface. Data obtained in this manner are in excellent agreement with theory (Fig. 6). Since the multiplying factor thus introduced applied to both calibration data and actual fracture toughness tests, there is no net error in crack length determination.

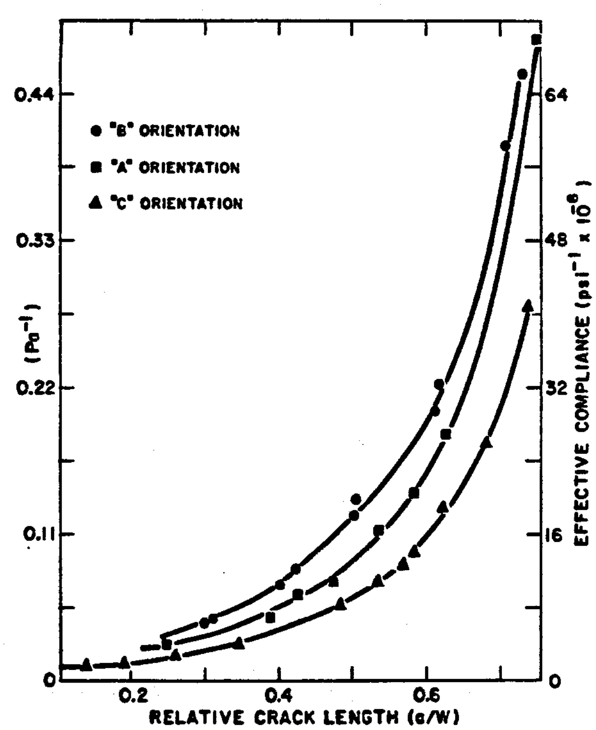

Figure 5. Compliance calibration curves for three orientations of Berkeley Granite (see Fig. 1).

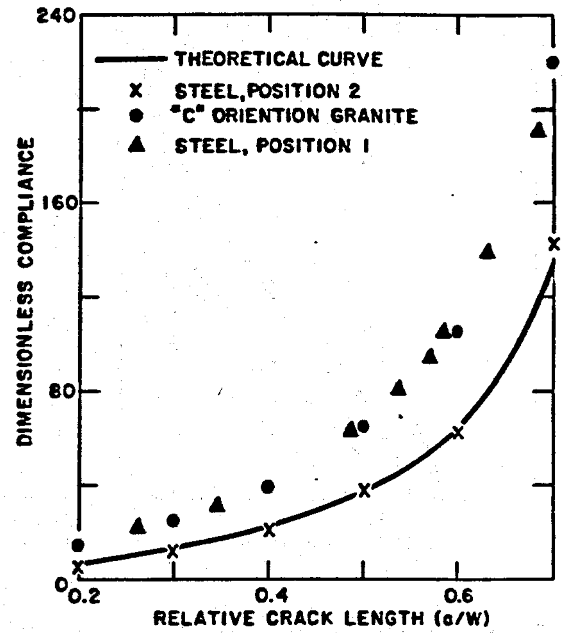

Figure 6. Comparison of compliance curves with the theoretical relation of Jones and Brown [6]. The solid line is the theoretical relation for the product C-E (compliance times Young's modulus). Triangles and circles are data for a steel sample and "C" orientation Berkeley Granite respectively. These data were taken with the LVDT in "position 1," 12.7 mm below the sample (see Fig. 2). The crosses are for the same steel specimen with LVDT mounted flush with the bottom surface of the sample (position 2).

The tensile moduli data (Table II) exhibit a pronounced orientation dependence. Samples stressed perpendicular to the polished surface show the highest values. The polished surface, or face C, is the "hardway" or "headgrain" plane, terms used in quarrying to describe the direction most resistent to splitting. (The other two naturally orthogonal faces, A and B, are the "grain" and "rift" planes respectively, the latter indicating the easiest splitting direction). Similar orientation effects have been observed in compressive moduli measurements on Chelmsford Granite by Peng and Johnson [7] and Todd et al. [8]. The present data also correspond to the orientation dependence of compliance calibration data in Fig. 5. From these observations, one would expect the rift plane to lie perpendicular to the lowest modulus sample, i.e. B orientation.

Calculation of apparent fracture toughness is based on the application of linear elastic fracture

TABLE III

FRACTURE TOUGHNESS, K_Q, VALUES FOR BERKELEY GRANITE

Sample Orientation	Number of Samples	Number of data Points	Average K_Q (MPa $\sqrt{m}$)	Standard Deviation (MPa $\sqrt{m}$)	Average K_Q (ksi $\sqrt{in.}$)	Standard Deviation (ksi $\sqrt{in.}$)
A	4	44	1.54	0.09	1.40	0.08
B	10	41	1.10	0.11	1.00	0.10
C	5	40	1.99	0.10	1.81	0.09

mechanics (LEFM), which is justified by the results on Westerly Granite by Schmidt and Lutz [10]. They found $K_Q = 2.6 \pm 0.1$ MPa $\sqrt{m}$ (2.4 ± 0.09 ksi $\sqrt{in.}$) using both the LEFM and J-integral methods. Measured values of K_Q are even lower for Berkeley Granite which allows the LEFM approach to be employed with even more confidence.

The procedure for calculating K_Q is based on ASTM E399-78[9], wherein

$$K_Q = (P_Q L/bW^{3/2}) \cdot f(a/w)$$

where P_Q is the critical load, L, b, a, and W are dimensions shown in Fig. 2 and f(a/W) is a semi-empirical function given as a polynomial. The load chosen for determination of K_Q was the maximum load during each cycle, because of difficulty in applying the ASTM secant-slope technique to the nonlinear load vs. COD curves for this granite. This procedure results in a slightly higher (~3%) values than the ASTM procedure. Because of the modified ASTM procedure and lack of reliable standards for establishing minimum specimen size in rocks, our values are reported as "apparent."

Average values of fracture toughness for each orientation are given in Table III. Again, a pronounced orientation effect is present. The toughest samples are "C" orientation, with fracture growing in the plane of the polished face. This is expected since that direction in the "head grain" as described for the tensile modulus data. Also, as predicted from the tensile data, "B" samples are indeed the weakest and the B surface of the block is thus the rift direction.

The only other K_Q values for granite in the literature besides Schmidt and Lutz [10], are those for Chelmsford Granite by Peng and Johnson [7] and for Barre Granite by Wilkening [9]. Values for the former ranged from 0.59 - 0.64 MPa $\sqrt{m}$ (0.54 - 0.58 ksi $\sqrt{in.}$) and exhibited virtually no orientation dependence. This latter observation is surprising because of the large orientation dependence of elastic modulus found in Chelmsford Granite. Peng and Johnson, however, used bend specimens in which the crack started directly from a wire sawn notch which is generally much less reliable than using a pre-cracked specimen as was done by Schmidt and Lutz [10] and in the present work.

Wilkening [11] also grew cracks from a precut notch in his J-integral measurements on Barre Granite. Although the data scatter is very wide, and no elastic modulus data are given, some qualitative indication of orientation effect can be seen. Using average values for tensile modulus (17.5 GPa) and Poisson's ratio (0.23) from Krech et al. [12], we obtain K_Q values ranging from .95 to 1.48 MPa $\sqrt{m}$ with mean of 1.17 MPa $\sqrt{m}$ and standard deviation of 0.15 MPa $\sqrt{m}$. This is in good agreement with our data for "B" orientation Berkeley.

The present results, those of Schmidt and Lutz [10] for Westerly Granite and the data of Wilkening [11] and Krech et al. [12] for Barre Granite combine to produce an empirical relationship between tensile modulus and fracture toughness. A plot of K_Q vs. E produces a smooth curve (Fig. 7) which covers all the data points. The relationship holds for three different rocks, for different orientations of the same rock and for data obtained by different techniques. Although a complete theoretical justification of this

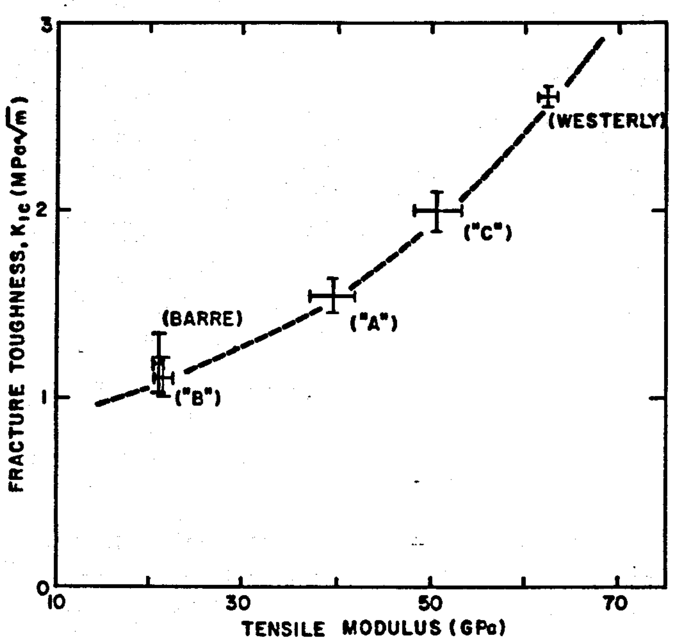

Figure 7. Relationship between tensile modulus and fracture toughness for granites. Data include Westerly Granite (Schmidt and Lutz [10]), Barre Granite (Wilkening [11]), and A, B, and C orientations of Berkeley Granite (present work). Error bars represent one standard deviation from the mean values.

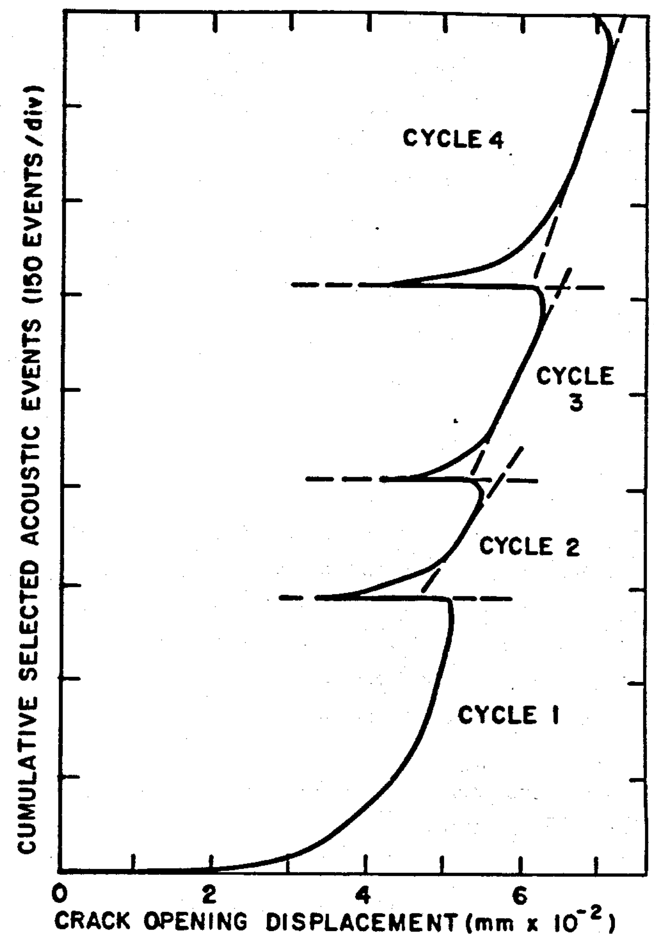

Figure 8. Acoustic emission for load cycles shown in Fig. 3. The straight portions represent steady crack growth rate and the dark circles are estimates of the onset of crack growth obtained by extrapolation. The values of COD thus obtained are also shown in Fig. 3 and correspond to critical load.

relationship is currently lacking, it does hold promise as a predictive tool for determining fracture toughness from modulus data alone.

The attempts made during these tests to use acoustic emission as a tool to detect the onset of crack growth were also encouraging. In Fig. 8, cumulative low frequency events vs. COD are plotted for the four successive cycles shown in Figure 3. These data are for a "B" orientation sample, the crack growing in the rift plane. For each cycle, data was recorded until maximum load was reached, indicating steady crack growth, then gated during unloading until compression was resumed for the next cycle. For each cycle after the first, the rate of events increases with crack opening until a steady rate is reached. This steady rate corresponds to steady crack growth under constant load line displacement rate. As shown in Figure 8, the point at which this steady growth commences can be estimated by extrapolating the constant emission rate portion of the curve back to the start for each cycle. The difference between the extrapolated straight line and the actual curve represents acoustic emission due to reopening the existing crack.

The COD values which correspond to the onset of steady crack growth have been replotted on Fig. 3. These values correspond to load levels slightly below the peak and thus are analagous to the ASTM method of obtaining P_Q. Where such data is available for all samples tested, it may be advantageous to use this point as the failure load in calculating K_Q.

Suzuki et al. [13] have made a similar proposal based on observation of distinctive frequency spectra of emission during crack growth in sandstones. Using a frequency analyzer, it was found that crack growth is accompanied by high frequency (1 MHz) events compared to the lower frequency (<100 KHz) events that occur during reopening of existing cracks.

We have attempted to simplify this process by filtering data into two frequency ranges and observing the ratio as a function of K/K_Q. Data were collected for different portions of successive loading cycles as described above (Fig. 4). The heavy portions of each cycle show the region over which data were collected. The dark circle is the median load of the data collection range which was divided by the peak load for that cycle to obtain a variable corresponding to the relative stress intensity factor. A value of 1.0 represents the critical load for which steady crack growth occurs.

The best data are shown in Figs. 4 and 9. A sharp maximum is seen in the ratio of high frequency to low frequency counts for $K = K_Q$, corresponding to steady crack growth. This is consistent with Suzuki, et al. observations [13], but the technique is unreliable and needs considerable refinement.

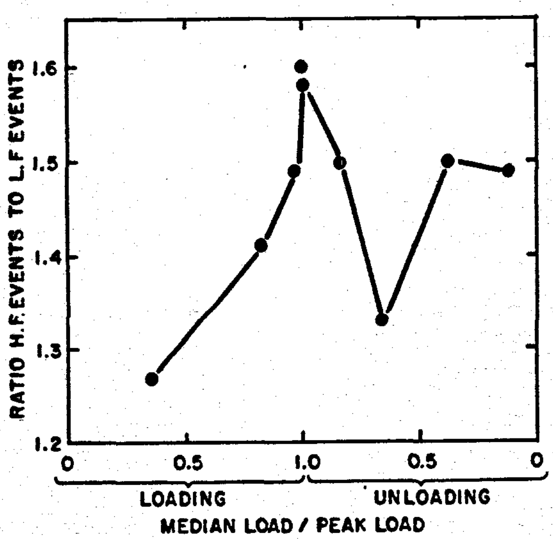

Figure 9. Frequency ratio as a function of relative load. The ratios of high- to low-frequency counts obtained for the experiment in Fig. 4 are plotted vs. the relative load. The median load was divided by the peak load so that a value of 1.0 represents load during steady crack growth. Values to the right of 1.0 represent data taken during unloading. A sharp increase in high frequency emission is seen during crack growth.

CONCLUSIONS

We have observed marked orientation dependence in both tensile modulus and fracture toughness in Berkeley Granite. A monotonic relationship exists between the two parameters which holds for the present data as well as for literature data on Westerly and Barre Granites. These observations have important consequences in HDR geothermal energy and other geo-engineering applications. The orientation of hydrofractures at depth may be influenced as much by anisotropic fracture toughness as by in situ stresses. In addition, it may be possible to predict K_Q from moduli measurements alone. Acoustic emission shows promise as a technique for estimating the critical load needed to calculate fracture toughness.

ACKNOWLEDGMENT

The financial support of the Division of Geothermal Energy of the U.S. Department of Energy is gratefully acknowledged. We are also indebted to K. Spicochi, D. Mann, and R. Anderson, and B. Hahn for their technical support and J. Blacic, R. Riecker, J. Petrovic and J. Tester for helpful discussions of the text.

REFERENCES

1. Cummings, R. G., Morris, G. E., Tester, J. W., and Bivins, R. L., 1979, "Mining Earth's Heat: Hot Dry Rock Geothermal Energy," Technology Review 81 (4), 1-19.

2. Smith, M. C., Potter, R. M., Aamodt, R. L., and Brown, D. W., 1975, "Man-Made Geothermal Reservoirs," Second United Nations Geothermal Energy Symposium, San Francisco, Calif., 1781-1787.

3. Eddy, A., 1978, Private communication.

4. Sykes, M. L., 1979, Private communication.

5. Schmidt, R. A., 1975, "Fracture Toughness Testing of Rock," Closed Loop, 5(2), 3-12.

6. Jones, M. H., Brown, W. F., 1970, "The Influence of Crack Length and Thickness in Plane Strain Fracture Toughness tests," in Review of Development in Plane Strain Fracture Toughness Testing, ASTM STP 463, American Society for Testing and Materials, 63-101.

7. Peng, S., Johnson, A. M., 1972, "Crack Growth and Faulting in Cylindrical Specimens of Chelmsford Granite," Int. J. Rock Mech. Min. Sci. 9, 37-86.

8. Todd, T., Simmons, G., Baldridge, W. S., 1973, "Acoustic Double Refraction in Low Porosity Rocks," Bull. Seis. Soc. Am. 63, 2007-2020.

9. "Standard Test Method for Plane-Strain Fracture Toughness of Metallic Materials (ANSI/ASTM 399-78)," 1978, 1978 Annual Book of Standards, Am. Soc. for Testing and Matls., Phil., PA.

10. Schmidt, R. A., Lutz, T. J., 1979, "K_{1C} and J_{1C} of Westerly Granite - Effects of Thickness and in-Plane Dimensions," Fracture Mechanics Applied to Brittle Materials, ASTM STP 678, S. W. Freiman, Ed., Am. Soc. for Testing and Matls., 166-182.

11. Wilkening, W. W., 1978, "J-Integral Measurement in Geological Materials," Proc. 19th U.S. Symp. on Rock Mech., Stateline, Nev., 1-3 May 1978, v. 1, 254-258.

12. Krech, W. W., Henderson, F. A., Hjelmstad, K. E., 1974, "A Standard Rock Suite for Rapid Excavation Research," U.S. Bur. Mines Report BM-RI-7865 m, 4-6.

13. Suzuki, M., Abe', H., Takahashi, H., Tamakawa, K., Kikuchi, M., 1978, "Acoustic Emission Characteristics and Fracture Toughness of Sandstone," Tech. Rpts., Tohoku University, 43, 231-240.